



## Convection in ice I shells and mantles with self-consistent grain size

Amy C. Barr<sup>1,2</sup> and William B. McKinnon<sup>1</sup>

Received 23 June 2006; revised 30 August 2006; accepted 26 September 2006; published 27 February 2007.

[1] The viscosity of ice I is grain size dependent for temperature and stress conditions appropriate for ice I shells and mantles of large and midsized icy satellites. Satellite thermal evolution, heat flux, critical shell thickness for convection, brittle/ductile transition temperature, and potential for surface deformation are therefore grain size dependent. Using measured grain sizes from terrestrial ice sheets experiencing temperature and strain rate conditions similar to convecting ice shells in icy satellites, we develop two end-member models of grain size and its evolution. In the absence of non-water ice impurities, grain size in a convecting ice shell of a large icy satellite will evolve over time to an equilibrium value, which we determine to be between 30 and 80 mm, because of dynamic recrystallization. Such large grains imply viscous ice, so convection in an ice shell thinner than 35 km in a large icy satellite such as Ganymede and Callisto would be sluggish at best and may cease after a few convective overturns (if it starts). Soluble ions and silicate microparticles may keep grains small, however, of order 1–5 mm, and permit convection in shells as thin as 30 km in large icy satellites. The dynamic recrystallization model provides a plausible upper limit on grain size in a geodynamically evolved ice shell, whereas grain sizes from dust-contaminated terrestrial ice cores provide a plausible lower limit on grain size in an icy satellite. On the basis of these constraints, grain sizes in evolved ice shells of large water ice satellites, in the absence of tidal forcing, should be of order 1 mm to 10 cm.

**Citation:** Barr, A. C., and W. B. McKinnon (2007), Convection in ice I shells and mantles with self-consistent grain size, *J. Geophys. Res.*, 112, E02012, doi:10.1029/2006JE002781.

### 1. Introduction

[2] Understanding heat transfer in the outer ice I shells and/or layers of large to midsized icy satellites is of key importance to satellite studies. The efficiency and mode of heat transport across their outer shells controls the global evolution of their interiors and styles of endogenic resurfacing. Our understanding of the geodynamic and thermal evolution of icy satellites is limited in part by our knowledge of how ice in their interiors behaves in response to applied stress.

[3] Laboratory experiments seeking to clarify the ductile behavior of ice I in terrestrial and planetary contexts suggest that, similar to terrestrial rock-forming minerals, strain in ice I is accommodated by several microphysical deformation mechanisms [Goldsby and Kohlstedt, 2001; Durham and Stern, 2001]. The total strain rate in ice as a function of stress and temperature is the sum of the strain rates from volume diffusion (*diff*), non-Newtonian grain-size-sensitive creep (*GSS*), which may occur as a result of

grain boundary sliding accommodated by basal slip [Goldsby and Kohlstedt, 2001; Durham and Stern, 2001; Goldsby and Kohlstedt, 2002], and dislocation creep (*disl*) [Goldsby and Kohlstedt, 2001],

$$\dot{\epsilon}_{total} = \dot{\epsilon}_{diff} + \dot{\epsilon}_{GSS} + \dot{\epsilon}_{disl}. \quad (1)$$

At low-to-moderate stresses associated with thermal convection in large icy satellites such as Ganymede and Callisto, ~1–100 kPa, deformation is likely accommodated by volume diffusion and grain-size-sensitive creep [Barr and Pappalardo, 2005; McKinnon, 2006]. When either volume diffusion or GSS accommodate strain in ice, the strain rate in and effective viscosity of ice are grain size dependent.

[4] Because the viscosity of ice is grain size dependent, grain size and its evolution control key aspects of the geodynamic and thermal evolution of the satellites. Grain size controls the onset, duration, and efficiency of convection in the satellites' interiors. In tidally flexed satellites such as Europa and Enceladus, grain size may control the spatial distribution of tidal heating in the ice shell provided viscous deformation in the warm ice during each tidal forcing cycle is accommodated by a grain-size-sensitive creep mechanism. Grain size also plays a key role in controlling the style of surface deformation on icy satellites by controlling the depth to the brittle/ductile transition. In

<sup>1</sup>Department of Earth and Planetary Sciences and McDonnell Center for the Space Sciences, Washington University in Saint Louis, Saint Louis, Missouri, USA.

<sup>2</sup>Department of Space Studies, Southwest Research Institute, Boulder, Colorado, USA.

this paper we restrict our discussion to ice I shells and mantles such as potentially created by differentiation in midsized icy satellites [Schubert *et al.*, 1986], or floating above internal aqueous layers (oceans) in large icy satellites [Schubert *et al.*, 2004].

[5] Ice grain size in icy satellite interiors is not well constrained. Modern studies of icy satellite convection have either implicitly assumed a grain size for ice I by considering the melting point viscosity to be a free parameter, typically  $\sim 10^{13}$  to  $10^{15}$  Pa s [Deschamps and Sotin, 2001; Tobie *et al.*, 2003; Spohn and Schubert, 2003; Mitri and Showman, 2005], or explicitly assumed a range of grain sizes, usually around a millimeter [McKinnon, 1999; Ruiz and Tejero, 2003; Barr *et al.*, 2004; Barr and Pappalardo, 2005; McKinnon, 2006]. Available estimates of ice grain size are focused on Europa, the most heavily studied icy satellite so far. Because the heat flux across the ice I shell of Europa depends on grain size, equating estimates of tidal and radiogenic heating within Europa to the convective and conductive heat flux suggests that the ice grain size is less than a few millimeters [Moore, 2006], and that deformation is accommodated by volume diffusion. This presumes the relatively strong tidal forcing has no effect on the convection except through the tidal heating term, which we doubt [McKinnon, 1999]. (Tidal effects, however, will be discussed in a future paper.) Constraints on the viscosity at the base of Europa's ice shell based on spacing between lenticulae on its surface had previously suggested that the grain size may be just a few microns there [Nimmo and Manga, 2002]. In contrast, simple models of ice grain growth over time suggest that grain size in Europa's shell could reach a few tens of meters near its base [Schmidt and Dahl-Jensen, 2003]. It has also been suggested that tidal flexing of Europa's ice shell may keep the grain size close to 1 mm [McKinnon, 1999]. These estimates do not place tight constraints on ice grain size, nor do they take into account the effects of processes known to affect grain size in terrestrial ice sheets, such as dynamic recrystallization and the presence of non-water impurities. As a result, ice grain size is necessarily considered a free parameter in nearly all studies of icy satellite thermal and geodynamic evolution.

[6] Observations of grain size, and the processes that control grain size in terrestrial ice sheets may shed light on grain size and its evolution in the outer ice I shell of a large to midsized icy satellite. We show below that temperature, stress, and strain rate conditions in polar ice sheets (e.g., the Greenland Ice Sheet) [De La Chapelle *et al.*, 1998; Thorsteinsson *et al.*, 1997] are not dissimilar to conditions expected within the outer ice I shells of large to midsized icy satellites. Grain size within terrestrial ice sheets is controlled by the concentrations of non-water ice impurities and by a process called dynamic recrystallization, where the average grain size of a polycrystalline material is modified as strain accumulates. Here, we use measured grain sizes, observations of the microphysical texture of ice, the laboratory-derived flow law for ice I, and a description of microphysical processes occurring during dynamic recrystallization in polycrystals to generate a rheologically and microphysically self-consistent model of grain size in a convecting ice shell. We use grain sizes and observations of the microstructure of ice in the GRIP ice

core from Greenland to constrain the governing parameters of our grain size model before extrapolating to conditions appropriate for the icy satellites. Using scaling relationships between the rheological parameters, convective heat flux, and convective velocities, we determine the equilibrium recrystallized grain size in a convecting ice shell and characterize how this grain size changes as a function of ice shell thickness and surface and basal temperature. We characterize the convective heat flux and timescale for convective turnoff in an ice shell where grain sizes evolve because of dynamic recrystallization.

[7] Grain sizes predicted by our dynamic recrystallization model are somewhat large on average (tens of millimeters), in contrast with the several-millimeter-sized grains typically observed in terrestrial ice sheets. In polar ice sheets formed from snow deposited during the last glacial maximum, grains are kept at a constant size of order 1 mm because of impurities that slow grain growth. We use grain sizes measured in dirty/salty terrestrial ice cores to estimate grain sizes in dirty and/or salty ice shells. If impurities control ice grain size, grain sizes should be approximately uniform in the ice shell. We determine how the likely presence of impurities might modify the conditions where convection can occur in the icy satellites, the convective heat flux, and the amount of impurities required to realize these modifications.

[8] We consider the dynamic recrystallization and impurity-bearing ice grain size models to be two end-member cases. The large grain sizes arising from dynamic recrystallization in the absence of impurities provides an upper bound on likely grain sizes in geodynamically active ice I shells, and the impurity-bearing ice model provides a lower bound on likely grain sizes. We are thus able to constrain grain sizes in the ice I shells of geodynamically evolved satellites to be within  $\sim 1$  to 100 mm, a substantial improvement over the 8 orders of magnitude in uncertainty suggested by previous work.

## 2. Grain Size Evolution by Dynamic Recrystallization

[9] Processes that control grain size in polycrystalline materials are of great interest to materials scientists in addition to terrestrial and planetary geophysicists. A large volume of work exists describing grain size and its evolution in metals, alloys, rock-forming minerals, and ice (see Humphreys and Hatherly [2004] for discussion). Although many observations exist, few microphysical models have been developed, owing to the complexity of the processes that create and destroy relevant crystal defects (i.e., dislocations), and the methods by which dislocations migrate through crystals.

[10] In the process of dynamic recrystallization, the mean grain size of a polycrystalline material is modified as the material deforms. Observations of recrystallized grain size in deformed materials, including ice, suggest that the mean recrystallized grain size ( $d$ ) is proportional to the stress ( $\sigma$ ) as  $d \sim \sigma^{-m}$  where  $m \sim 1$  [Poirier, 1985; Derby, 1991; Humphreys and Hatherly, 2004]. The work of Shimizu [1998] seeks to explain this empirical observation with a model of the physical processes that result in grain size modification during deformation of materials at high tem-

**Table 1.** Rheological Parameters

Parameter	Value
<i>GSS Creep</i> <sup>a</sup>	
$A$ , $\text{m}^p \text{Pa}^{-n} \text{s}^{-1}$	$6.2 \times 10^{-14}$
$n$	1.8
$p$	1.4
$Q^*$ , $\text{kJ mol}^{-1}$	49
<i>GSS Creep + Dynamic Recrystallization</i>	
$b$ , $\text{m}$	$4.52 \times 10^{-10}$ <sup>a</sup>
$m$	1.25 <sup>b</sup>
$\mu$ , $\text{Pa}$	$3.5 \times 10^9$
$K$	13–21 <sup>c</sup>
$Q^*$ , $\text{kJ mol}^{-1}$	49
$A' = A/(b\mu^m K)^p$ , $\text{Pa}^{-n'} \text{s}^{-1}$	$(1.5 \times 10^{-17}) \times K^{-1.4}$
$n' = n + mp$	3.55

<sup>a</sup>From *Goldsby and Kohlstedt* [2001].

<sup>b</sup>From *Shimizu* [1998].

<sup>c</sup>Obtained by fitting grain sizes in the GRIP core (see section 2.1).

peratures. *Shimizu* [1998] suggests that the equilibrium recrystallized grain size in deformed materials is controlled by a balance between (1) grain growth and (2) formation of new grains (nucleation) by a process called subgrain rotation. In subgrain rotation, dislocations migrate toward grain boundaries at a flux that depends on the dislocation density. The dislocation density is controlled by the total stress experienced by the material, which, in an icy satellite, may be due to thermal convection, or thermal buoyancy plus tidal stresses, but deformation (likely, convective strain) is required to drive subgrain rotation. Therefore estimates of recrystallized grain size are reasonable only if the ice has experienced significant strain (i.e., beneath the stagnant lid of a convecting ice shell).

[11] The rate of grain growth is proportional to the diffusion coefficient at grain boundaries,  $D_{gb}$ , which is temperature dependent. Similarly, the rate of nucleation (formation of grain boundaries) is proportional to the self-diffusion coefficient,  $D_v$ , which is also temperature dependent. Balancing these two rates yields an expression for recrystallized grain size as a function of stress and temperature,

$$\frac{d}{b} = A_1 \left( \frac{\sigma}{\mu} \right)^{-m} \exp \left( - \frac{(Q_{gb} - Q_v)}{4k_b T} \right) \quad (2)$$

where  $b$  is Burger's vector for the material in question,  $\sigma$  is stress,  $\mu$  is the shear modulus,  $m = 1.25$  (and the factor of 4 on the r.h.s.) are appropriate for intracrystalline nucleation,  $Q_{gb}$  is the activation energy for grain boundary diffusion,  $Q_v$  is the activation energy for self-diffusion,  $k_b$  is Boltzmann's constant, and  $T$  is temperature. The constant  $A_1$  is related to properties of the ice crystal lattice and descriptive properties of the structure and behavior of grain boundaries, for example, the misorientation angle of subgrain boundaries, the critical misorientation angle between adjacent crystal lattices at which a new grain boundary forms, the Burger's vector for ice, and grain boundary width [*Shimizu*, 1998]. Laboratory measurements exist for some of the descriptive parameters included in  $A_1$ , but because diffusion in ice I has

not been observed in the laboratory (see *Goldsby and Kohlstedt* [2001] for discussion), we group these parameters into a constant  $K$  that will be determined empirically by fitting an equation similar to equation (2) to measured grain sizes in a terrestrial ice core. This procedure will be discussed in section 2.1.

[12] The value of recrystallized grain size depends on the ratio between  $D_{gb}$  and  $D_v$  (see equation (12) of *Shimizu* [1998]), which results in the exponential dependence on the difference ( $Q_{gb} - Q_v$ ) in equation (2). (If  $Q_{gb} = 2/3 Q_v$  [*Frost and Ashby*, 1982], the effective activation energy would be only  $5 \text{ kJ mol}^{-1}$ .) This value, relating grain size to temperature, can be determined through experiments at a range of different temperatures, but because equation (2) suggests that equilibrium grain size depends only weakly on temperature, this dependence is not well characterized and is commonly ignored [*Shimizu*, 1998].

[13] We will use a simplified version of equation (2) to model grain sizes in terrestrial ice sheets and icy satellites,

$$\frac{d}{b} = K \left( \frac{\sigma}{\mu} \right)^{-m}, \quad (3)$$

where  $K$  is a dimensionless parameter of order 10–100 [*Shimizu*, 1998]. Values of the descriptive parameters of our dynamic recrystallization model are summarized in Table 1.

[14] Glaciological literature often attributes grain size evolution in deforming ice to two different recrystallization processes, “rotation recrystallization,” where grain size is decreased by subgrain rotation without subsequent grain growth, and “migration recrystallization,” where both grain growth and subgrain rotation occur. It has been suggested, however, that rotation recrystallization is merely a transient regime of grain size evolution that occurs in deformed materials as they approach the equilibrium state where grain growth occurs during recrystallization [*Poirier*, 1985; *Shimizu*, 1998]. Here, we model grain sizes due to migration recrystallization because grain growth and nucleation acting together in this process lead to a steady state grain size.

## 2.1. Application of Grain Size Model to GRIP

[15] The GRIP ice core samples 3030 m of ice from the Greenland Ice Sheet extending  $\sim 100$  kyr in the past [*Thorsteinsson et al.*, 1997]. Figure 1 illustrates the grain size profile in the GRIP ice core using data gathered by *De La Chapelle et al.* [1998]. In the top 650 m of the GRIP core (not shown in Figure 1) ice grains grow with time as [*Poirier*, 1985]

$$d^2 = d_o^2 + kt \quad (4)$$

where  $d$  is grain size,  $d_o$  is the initial grain size,  $t$  is time, and the growth rate  $k = 1.2 \times 10^{-16} \text{ m}^2 \text{ s}^{-1}$  [*De La Chapelle et al.*, 1998].

[16] Between a depth of 650 m and 1625 m, the ice grain size is 4 mm and is constant as a function of depth. This portion of the GRIP core, deposited during the present (Holocene) interglacial period, has low concentrations of non-water ice impurities, so grain boundaries are free to migrate, resulting in rapid grain growth. Yet, the grain size



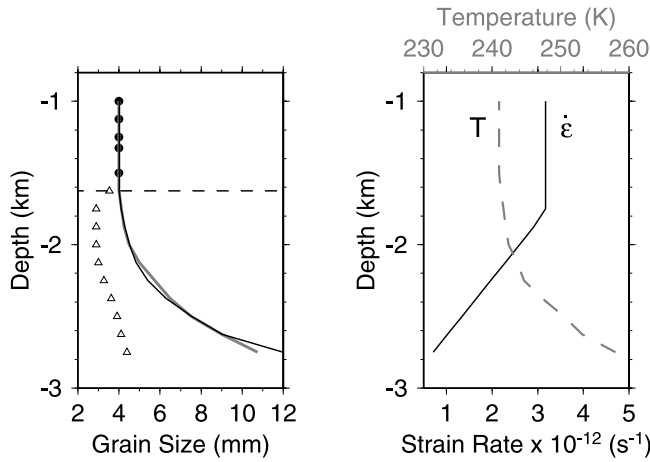


**Figure 1.** (left) Grain sizes in the GRIP ice core, where solid circles represent values of ice grain size measured in relatively impurity-free interglacial ice (younger than 18,000 years) and triangles represent grain size measurements in relatively impurity-laden glacial period ice. The horizontal dashed line indicates the boundary between the young, shallow, interglacial ice and deeper glacial ice. The gray line indicates a fit to the interglacial ice data from *De La Chapelle et al.* [1998] and their theoretical model of grain size due to dynamic recrystallization. The black line indicates our fit to the interglacial ice grain sizes and model of *De La Chapelle et al.* [1998] assuming that strain in the core is accommodated by grain-size-sensitive creep and grain size is proportional to  $\sigma^{-1.25}$ , as suggested by the analysis of *Shimizu* [1998]. Mismatch between either model and the data below a depth of 1625 m indicates that impurities control ice grain size in this portion of the core. (right) Vertical strain rate in the ice core (black line) and temperature (gray dashed line) are key inputs to our grain size model and are obtained from *Thorsteinsson et al.* [1997].

in this portion of the core remains constant as a function of depth (equivalently, time). It has been suggested that the accumulated strain due to vertical layer compaction results in grain size reduction due to dynamic recrystallization [*De La Chapelle et al.*, 1998]. Here, we apply the dynamic recrystallization model of *Shimizu* [1998] and the GSS flow law from *Goldsby and Kohlstedt* [2001] to explain the grain sizes observed in the GRIP core. We fit our model to the measured grain sizes in GRIP to constrain the governing parameters. Having determined how grain sizes in GRIP depend on temperature and strain rate, we then use the model to extrapolate to planetary conditions to predict how grain size in icy satellite shells and mantles depend on temperature and strain rate.

[17] The fabric of the ice grains observed in GRIP suggests that the core experiences uniaxial compression between a depth of 650 m and 2800 m [*Thorsteinsson et al.*, 1997]. Horizontal shear is negligible because the core was obtained close to the ice divide where the surface slope is small ( $\leq 10^{-3}$ ) [*De La Chapelle et al.*, 1998]. A simple model of layer thinning due to vertical compaction

suggests that the vertical strain rate is a constant  $\sim 10^{-4} \text{ yr}^{-1}$  to a depth of  $\sim 1775$  m, and linearly decreases to zero at a depth of 3030 m [see *Thorsteinsson et al.*, 1997, and references therein]. The implied vertical strain rates in the core,  $\sim 3 \times 10^{-12} \text{ s}^{-1}$  near the surface to  $\sim 7 \times 10^{-13} \text{ s}^{-1}$  at a depth of 2800 m, are similar to estimates of convective strain rates in the outer ice I shells of large icy satellites such as Callisto [*McKinnon*, 2006]. On the basis of the observations of grain size and texture in the GRIP core, the threshold strain where grains reach equilibrium sizes predicted by dynamic recrystallization is  $\sim 25\%$  [*Thorsteinsson et al.*, 1997].

[18] The temperature in the ice core is constant at  $-32^\circ\text{C}$  (241 K) to a depth of 1800 m, and increases linearly to  $-9^\circ\text{C}$  (264 K) at a depth of 3030 m [*Thorsteinsson et al.*, 1997]. This range of temperatures is remarkably close to the temperatures expected in the convecting interior of an ice I shell (240 to 260 K), depending on shell thickness. At a depth of 2800 m where near-bed shear and large impurity levels begin to control the grain size, the temperature in the GRIP core is 258 K.

[19] The laboratory-derived rheology for ice I determined by *Goldsby and Kohlstedt* [2001] suggests that deformation within the majority of the GRIP core is accommodated by GSS creep [*Goldsby and Kohlstedt*, 2001], which may be accommodated by grain boundary sliding [*Goldsby and Kohlstedt*, 2002], and is weakly non-Newtonian and grain size dependent,

$$\dot{\epsilon} = \frac{A}{d^p} \sigma^n \exp\left(\frac{-Q^*}{RT}\right) \quad (5)$$

where  $A$  is the pre-exponential constant,  $p$  is the grain size exponent,  $n$  is the stress exponent,  $Q^*$  is the activation energy,  $R$  is the gas constant, and  $T$  is temperature. Measured values of the rheological parameters used for GSS creep are summarized in Table 1.

[20] Combining the ice flow law (equation (5)) and the expression for recrystallized grain size from *Shimizu* [1998] (equation (3)) yields a relationship between the grain size, strain rate, and temperature in the core,

$$d = (bK\mu^m)^{\frac{n}{n+mp}} \left(\frac{A}{\dot{\epsilon}}\right)^{m/(n+mp)} \exp\left(\frac{-mQ^*}{(n+mp)RT}\right). \quad (6)$$

With knowledge of the temperature and strain rate as a function of depth, the only unknown in the expression for the recrystallized grain size is the constant  $K$ . Figure 1 (left) illustrates the grain size as a function of temperature for the GRIP ice core, and shows our fit to the grain sizes in interglacial ice (above 1625 m) using equation (6) which gives  $K = 17.8 \pm 4$ . Included in our fit is the theoretical ice grain size profile for the GRIP core in the absence of impurities calculated by *De La Chapelle et al.* [1998], which was obtained by assuming that ice below a depth of 1625 m in the GRIP core behaved in a similar fashion to ice between 650 m and 1625 m. The mismatch at depth between the modeled grain sizes and the measured ice grain sizes in Figure 1 indicates that the presence of nonwater ice impurities keeps the grains smaller than predicted by

dynamic recrystallization. We will discuss this further in section 3.

## 2.2. Equilibrium Recrystallized Grain Size in a Convecting Ice Shell

[21] To obtain estimates of the equilibrium recrystallized grain size in a convecting ice shell, we evaluate the ice grain size in the GSS creep flow law (equation (5)) using the expression for recrystallized grain size from *Shimizu* [1998] to obtain a modified flow law for ice where the grain size due to dynamic recrystallization is implicitly and self-consistently determined [*Solomatov*, 2001; *Rainey and Stevenson*, 2005],

$$\dot{\epsilon} = \frac{\sigma^{n+mp} A}{(Kb\mu^m)^p} \exp\left(\frac{-Q^*}{RT}\right). \quad (7)$$

In this modified rheology, the effective stress exponent is

$$n' = n + mp, \quad (8)$$

or 3.55 for GSS creep, and the reduced pre-exponential constant is

$$A' = \frac{A}{(Kb\mu^m)^p}. \quad (9)$$

With these definitions, the GSS ice flow law can be rephrased as

$$\dot{\epsilon} = \sigma^{n'} A' \exp\left(\frac{-Q^*}{RT}\right). \quad (10)$$

The effective viscosity of the ice,  $\eta_{eff} = \sigma/3\dot{\epsilon}$ , is non-Newtonian with stress exponent  $n'$  and activation energy  $Q^*$  [*Rainey and Stevenson*, 2005],

$$\eta_{eff} = \frac{1}{3A'^{1/n'}} \dot{\epsilon}_{II}^{(1-n')/n'} \exp\left(\frac{Q^*}{n'RT}\right), \quad (11)$$

where  $\dot{\epsilon}_{II}$  is the second invariant of the strain rate tensor. Values of rheological parameters used for the GSS + dynamic recrystallization rheology are summarized in Table 1.

[22] To estimate the mean recrystallized grain size in an ice I shell, we estimate the convective strain rate in the ice shell using scaling relationships between convective velocity, Rayleigh number, and rheological parameters derived by *Solomatov and Moresi* [2000]. The velocity in the interior of a convecting layer of non-Newtonian fluid is approximately

$$u_i \approx (0.046 + 0.007n') \frac{\kappa}{D} \left(\frac{Ra_i}{\theta}\right)^{\frac{2n'}{n'+2}}, \quad (12)$$

where  $Ra_i$  is the Rayleigh number evaluated at the interior viscosity and temperature, and  $\theta$  is the number of e-foldings in viscosity between the surface and base of the ice shell. (We use the less complex ‘‘velocity scaling I’’ of *Solomatov*

and *Moresi* [2000; V. S. Solomatov, personal communication, 2006].) We assume that  $Ra_i \sim Ra_1$ , the Rayleigh number at the base of the ice shell, which is defined as

$$Ra_1 = \frac{3A'^{1/n'} \rho g \alpha \Delta T D^{(n'+2)/n'}}{\kappa^{1/n'} \exp\left(\frac{Q^*}{n'RT_m}\right)}, \quad (13)$$

where  $\rho = 930 \text{ kg m}^{-3}$  is a representative density for convecting ice,  $\Delta T$  is the difference between the melting temperature of ice ( $T_m$ ) and the surface temperature of the satellite, ( $T_s$ ),  $g = 1.3 \text{ m s}^{-2}$  for Europa and representative of a large icy satellite (midway between values for Ganymede and Callisto),  $\alpha = 1.6 \times 10^{-4} \text{ K}^{-1}$  is the thermal expansion, and  $\kappa = 1.4 \times 10^{-6} \text{ m}^2 \text{ s}^{-1}$  is the thermal diffusivity (again, representative values). The value of  $\theta$  is related to the rheological parameters and melting temperature of ice using [*Solomatov and Moresi*, 2000]

$$\theta = \frac{1.2Q^* \Delta T}{RT_m^2}, \quad (14)$$

where the factor of 1.2 is included to approximately account for the difference between an Arrhenius temperature function and the Frank-Kamenetskii approximation [*Reese et al.*, 1999]. We find good agreement between numerically calculated values of the Nusselt number,  $Nu$  (the dimensionless heat flow),  $\theta$ , and  $Ra_i$  for the GSS + dynamic recrystallization rheology (discussed in section 2.4) and the scaling relationships including the factor of 1.2. (However, note that in this paper we will not consider the additional effects of shell curvature or temperature-dependent thermal conductivity on  $\theta$ . For a detailed discussion, see *McKinnon* [2006].)

[23] The interior strain rate is estimated using

$$\dot{\epsilon}_i \sim \frac{u_i}{D - \delta_L} \sim \frac{u_i Nu}{D} \quad (15)$$

where  $\delta_L$  is the thickness of the stagnant lid and is approximated using  $\delta_L/D \sim Nu^{-1}$ . The Nusselt number is related to the interior Rayleigh number and  $\theta$  by the scaling relationship [*Solomatov and Moresi*, 2000]

$$Nu = (0.31 + 0.22n') \theta^{\frac{2(n'+1)}{n'+2}} Ra_i^{\frac{n'}{n'+2}}. \quad (16)$$

[24] Combining the  $Nu$  and  $u_i$  scalings yields an approximate relationship between the estimated convective strain rate, Rayleigh number, and  $\theta$ ,

$$\dot{\epsilon}_i \sim (0.046 + 0.007n')(0.31 + 0.22n') \frac{\kappa}{D^2} Ra_i^{\frac{3n'}{n'+2}} \theta^{-\frac{2(2n'+1)}{n'+2}}. \quad (17)$$

Substituting this expression for the strain rate in equation (6) and evaluating the temperature at  $T = T_i \sim T_m$  allows

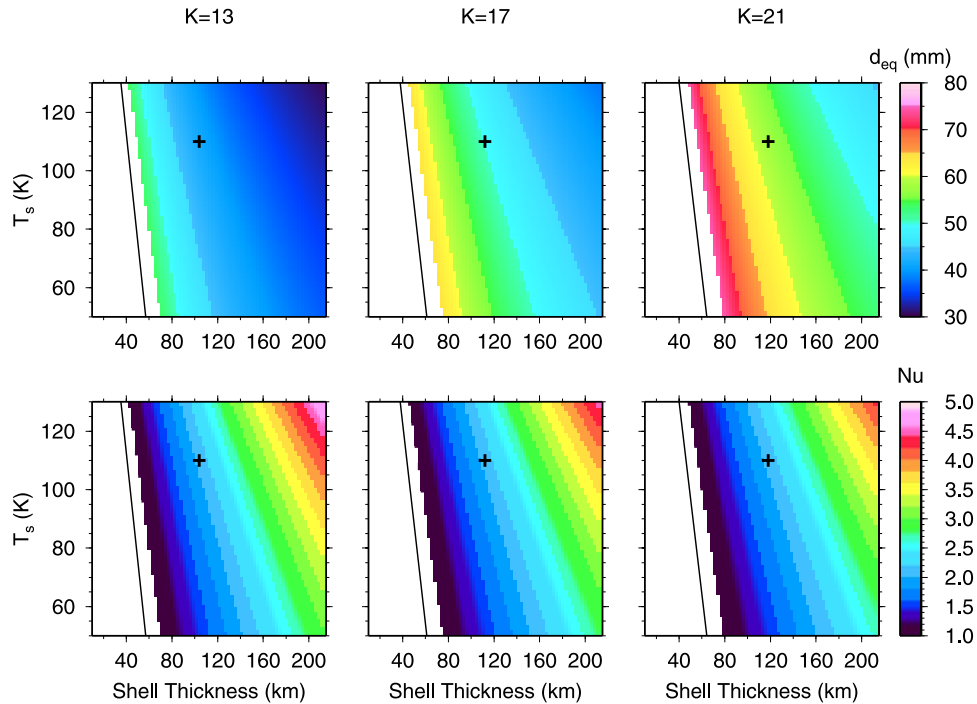


**Figure 2.** (top) Equilibrium recrystallized grain size ( $d_{eq}$  (mm)) as a function of surface temperature  $T_s$  (K) and ice shell thickness for a range of temperatures and shell thickness values appropriate for large icy satellites. The constant  $K$  that controls the recrystallized grain size is varied from  $K = 13$  (left graph) to  $K = 17$  (middle graph) to  $K = 21$  (right graph) to illustrate how a modest increase or decrease in  $K$  can yield grain sizes a factor of  $\sim 1.5$  larger or smaller. Black lines show the critical ice shell thickness for convection as a function of surface temperature for that particular value of  $K$  (see Figure 4); offsets are discussed in section 2.6.2. Crosses on each graph represent the location of the simulation shown in Figure 3 in the  $T_s, D$  parameter space. (bottom) Convective heat flux ( $Nu$ ) as a function of surface temperature and ice shell thickness. For a wide range of parameters, convection is sluggish ( $1 < Nu < 5$ ) because ice grain sizes predicted by dynamic recrystallization are relatively large (30–80 mm).

estimates of the mean equilibrium recrystallized grain size in the convecting interior.

[25] The scaling relationships in equations (12) and (16) were developed principally for vigorously convecting systems where the convective flow field and heat flux are time dependent [Solomatov and Moresi, 2000]. For non-Newtonian rheologies of high enough  $n$ , this scaling relationship provides a good approximation to the behavior in the lower  $Nu$ , steady state regime as well, and which occupies a small portion of  $Ra-Nu-\theta$  space for icy satellites in any case. (See Figure 13 of Dumoulin *et al.* [1999] for a comparison between the two scaling relationships for  $n = 3$ .)

### 2.3. Mean Grain Size

[26] Figure 2 illustrates the variation in grain size as a function of ice shell thickness, which controls  $Ra_1$ , and surface temperature, which controls both  $Ra_1$  and  $\theta$  for values of  $K = 13, 17$  and  $21$ , chosen to demonstrate how modest variations in  $K$  control variations in mean grain size in the convecting interior. For  $K = 13$ , the mean equilibrium grain size in an ice shell 100–150-km-thick ranges between 35 and 48 mm, depending on the value of surface temperature, which controls the viscosity contrast between the cold surface ice and warm ice at the base of the ice shell, and thus, the vigor of convection. For larger values of  $K$ , the mean equilibrium grain size in the shell increases to values closer to 55 mm, achieved in sluggishly convecting ice

shells where convective strain rates are very slow. For a given value of  $K$ , the mean recrystallized grain size in the convecting interior decreases as convection becomes more vigorous. Small grains are expected in thicker ice shells with vigorous convection, and in shells with higher surface temperatures and correspondingly thinner stagnant lids.

[27] In order for grain sizes in the ice shell to be approximated by the dynamic recrystallization model we have discussed here, the grain size must equilibrate to the local temperature and strain rate conditions in the ice shell on a timescale much faster than the convective timescale ( $D/u_i$ ), or faster than  $\sim 10^5 - 10^7$  yr (note that  $D/u_i$  is independent of  $D$ ). Because ice grains in terrestrial sheets achieve equilibrium recrystallized grain sizes on timescales of  $\sim 10^4$  years, (i.e., at depths corresponding to 18,000-year-old ice in the GRIP core), we expect this condition to be met in icy satellite interiors. In addition, grain size estimates are valid only for the convective interior of the ice I shell where strain has exceeded a few tens of percent (e.g., 25%) on the convective timescale.

### 2.4. Spatial Variation of Grain Size Within the Ice Shell

[28] In a convecting ice shell, the equilibrium grain size will vary as a function of depth and horizontal position in the ice shell because of temperature and strain rate variations in the convective flow field. To illustrate the magni-

tudes of these variations, we simulate convection in an ice I shell with grain size implicitly evaluated using the GSS + dynamic recrystallization rheology described in section 2.2. We use the finite element convection model Citcom [Moresi and Solomatov, 1995; Moresi and Gurnis, 1996; Zhong et al., 1998, 2000; Barr et al., 2004] to calculate the convective flow field in a  $1 \times 1$  2D Cartesian box with  $64 \times 64$  elements. We use free-slip boundary conditions on the surface ( $z = 0$ ), base ( $z = -D$ ), and edges ( $x = 0, x_{\max}$ ) of the domain. We describe the viscosity of ice using the full Arrhenius temperature dependence (equation (11)). To ensure numerical stability, we also impose an upper viscosity cutoff of  $\eta_{\max} = 10^{10}\eta_o$ . Provided the viscosity cutoff is greater than  $\sim\eta_o \exp(4(n' + 1)) \sim 10^8\eta_o$ , which ensures that the numerical convection model can achieve viscosity values large enough for the stagnant lid to remain motionless, the outcome of the numerical model does not depend on the value of upper cutoff viscosity [Solomatov, 1995; Solomatov and Moresi, 2000].

[29] To characterize the mean grain size in a convecting ice shell, we use a definition that conforms to previous definitions of “averages” of spatially varying quantities within a convecting layer [Solomatov and Moresi, 2000]. The mean grain size we report for our numerical simulations is determined by evaluating the grain size using equation (6) with  $\dot{\epsilon} = \dot{\epsilon}_i$  and  $T = T_i$ , where  $\dot{\epsilon}_i$  is the maximum value of the second invariant of the strain rate tensor beneath the stagnant lid, and  $T_i$  are calculated a posteriori from our numerical results. Using this definition of mean grain size, the grain sizes from our numerical simulations match the values predicted by the scaling relationships to within 10%. The agreement between the value of  $d$  predicted by the numerical calculation and the scaling relationships indicates that we can accurately estimate grain size in ice shells with a wide range of  $Ra$  and  $\theta$  values without the need to run time-consuming numerical simulations in every case.

[30] Figure 3 illustrates the variation of ice grain size in a shell  $\sim 85$  km thick, with a surface temperature of 110 K and melting temperature of ice of 260 K. Grain sizes are determined implicitly (using equation (6)), through numerical evaluation of the strain rate (specifically, the second invariant of the strain rate tensor) and temperature in each element. The mean grain size in the convecting interior is 40 mm if  $K = 13$ , 48 mm if  $K = 17$ , and 55 mm if  $K = 21$ . The grain size beneath the stagnant lid ranges from 1 mm to 120 mm and reflects the variations in temperature and strain rate in the convecting interior. The stagnant lid thickness is determined from the convective velocity field using the method of Solomatov and Moresi [2000, Figure 2]. Estimates of grain size are only applicable in regions of the ice shell where the strain has exceeded the threshold value of  $\sim 25\%$  over the convective timescale. We estimate strain as  $\epsilon = \dot{\epsilon}_{II}\tau_{diff}$  where  $\tau_{diff} = D^2/\kappa$ , and value of the second invariant of the strain rate tensor (at a given location) is determined from the outcome of our numerical simulation. Contours on each grain size map show the locations of approximately 0.1%, 1%, 10%, and 100% strain, which demonstrates that estimates of grain size are unphysically small in the stagnant lid because the ice shell has not experienced enough strain to reach the equilibrium recrystallized grain size.

## 2.5. Convective Heat Flux

[31] In the absence of tidal dissipation, we can estimate the heat flux across a convecting ice shell with the equilibrium grain size predicted by dynamic recrystallization using the scaling relationships from Solomatov and Moresi [2000]. Plots in the bottom row of Figure 2 illustrate the variation in  $Nu$  as a function of ice shell thickness, surface temperature, and  $K$ . Values of  $Nu$  are relatively small ( $< 5$ ), indicating sluggish convection, as suggested by the large grain sizes and viscous ice implied by our dynamic recrystallization model.

[32] Crosses on the plots of grain size and heat flux as a function of surface temperature and grain size in Figure 2 show the location of our numerical simulation (discussed in section 2.4) in terms of surface temperature and shell thickness. The value of  $Nu$  predicted by the scaling relationships for this value of ice shell thickness and surface temperature is approximately 1.65, very close to the numerically calculated value of 1.6. The agreement between our numerically calculated value of  $Nu$  and the value predicted by our scaling relationships is an illustration of the validity of the scaling relationships between  $Nu$ - $Ra$ - $\theta$  developed by, for example, Dumoulin et al. [1999] and Solomatov and Moresi [2000].

## 2.6. Can Convection Last?

[33] As demonstrated by Figures 2 and 3, grain sizes in the ice shells of the satellites are relatively large (30–80 mm) for a wide range of parameters appropriate for large, if not midsized, icy satellites. Owing to the grain-size-dependent viscosity, if convection began in an ice shell with a small grain size, the ice in the shell may become too stiff to convect as the mean grain size in the convecting interior of the shell reaches the equilibrium value predicted by dynamic recrystallization.

[34] Convection can occur in an ice I shell if the Rayleigh number at the base of the shell defined by equation (13) exceeds a critical value. To judge whether convection is possible in an ice shell where grain size has evolved because of dynamic recrystallization, we calculate the critical Rayleigh number for the non-Newtonian GSS + dynamic recrystallization rheology and compare this critical Rayleigh number to the basal Rayleigh number. We use this to determine the minimum ice shell thickness where convection can continue (cf. section 3.1).

### 2.6.1. Critical Rayleigh Number

[35] To determine the critical Rayleigh number for convection with a GSS + dynamic recrystallization rheology, we use the numerical method of determining  $Ra_{cr}$  for non-Newtonian fluids developed by Solomatov and Barr [2006]. In this method, the critical Rayleigh number is determined by finding the minimum value of  $Ra$  (for any convective aspect ratio) where the numerically determined value of  $Nu > 1$ . Figure 4 illustrates the variation in critical Rayleigh number obtained for the GSS + dynamic recrystallization rheology ( $n' = 3.55$ ,  $Q^* = 49$  kJ/mol). The critical Rayleigh number is calculated for a range of surface temperatures appropriate for ice I shells of large to midsized icy satellites, from  $\sim 45$  K to 130 K. The theory of Solomatov [1995] (where we use the definition of  $\theta$  in equation (14)) is used to interpolate between values of  $T_s$  or to extrapolate our results to higher or lower values of surface temperature.



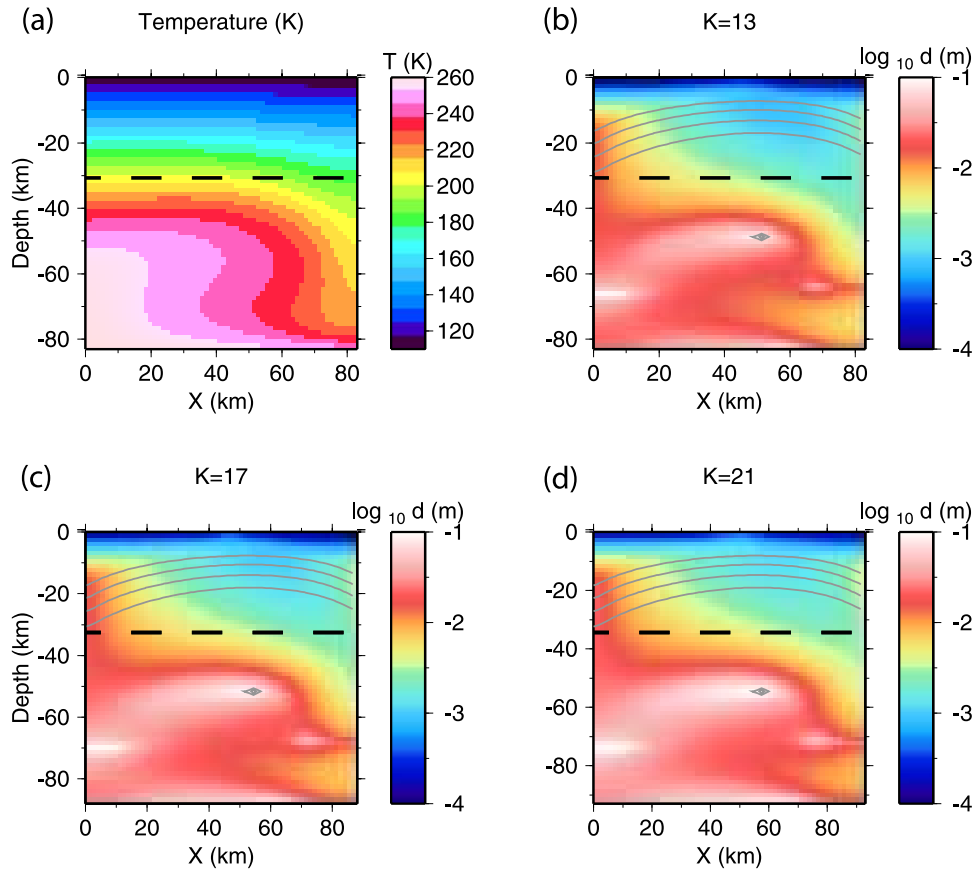


**Figure 3.** (a) Convective temperature field and equilibrium ice grain size due to dynamic recrystallization in a shell  $\sim 85$  km thick with  $T_s = 110$  K and  $T_m = 260$  K,  $Ra_1 = 2.1 \times 10^3$  with (b)  $K = 13$ , (c)  $K = 17$ , and (d)  $K = 21$ . The boundary of the stagnant lid, which is effectively mobile, is indicated by the thick dashed lines. Ice grain sizes in the convecting interior range from less than 1 mm to 120 mm, reflecting variations in strain rate and temperature in the ice shell. Grain size in the convecting interior ranges from 40 to 55 mm as a function of  $K$ . Estimates of grain size are only realistic in portions of the ice shell that have experienced sufficient strain. Gray contours indicate locations of approximate strain of 0.1%, 1%, 10%, and 100% within the stagnant lid over a diffusion time; these grain size estimates are unphysically small because the ice shell has not experienced enough strain for grain sizes to have reached the equilibrium grain size dictated by dynamic recrystallization.

Values of critical Rayleigh number range from  $1.8 \times 10^3$  for a surface temperature of 45 K to  $4.8 \times 10^2$  for a surface temperature of 130 K.

### 2.6.2. Minimum Ice Shell Thickness Where Convection Can Continue

[36] The minimum critical ice shell thickness where convection can continue is related to the critical Rayleigh number by ( $Ra_{cr,1}$ )

$$D_{cr} = \left( \frac{Ra_{cr,1} \kappa^{1/n'} \exp\left(\frac{-Q^*}{n'RT_m}\right)}{3A^{1/n'} \rho g \alpha \Delta T} \right)^{n'/(n'+2)}. \quad (18)$$

Figure 4 (right) shows the variation in minimum shell thickness for convection as a function of surface temperature for  $K$  values between 13 and 21, assuming the  $\kappa$ ,  $\rho$ ,  $g$ , and  $\alpha$  values used in section 2.2. The minimum shell thickness where convection can occur ranges from 32 km to 65 km, is inversely proportional to the surface temperature,

and increases by 10% as the value of  $K$  is increased 13 to 21. Because  $Ra_{cr,1}$  is derived for nonunity aspect ratio convection, the  $D_{cr}$  plotted in Figure 2 (and Figure 6) can be offset from the  $Nu = 1$  contours shown.

### 2.6.3. Timescale for Convective Turnoff

[37] Most of the values of  $D_{cr}$  are similar to the conductive ice shell thicknesses predicted for large-to-midsized icy satellites earlier in solar system history. This suggests that for convection to begin in the icy satellites, ice grain sizes must be initially very small. If convection were to begin, convection would cease when the grains in the warm convecting interior of the ice shell (beneath the stagnant lid) reach their equilibrium recrystallized values. The timescale for the grains to reach the equilibrium value is the timescale over which ice in the convecting sublayer has achieved a strain of, say,  $\sim 25\%$ , or

$$\tau_{equilib} \sim \frac{0.25}{\dot{\epsilon}_i} \sim 0.25 \frac{D}{u_i}. \quad (19)$$



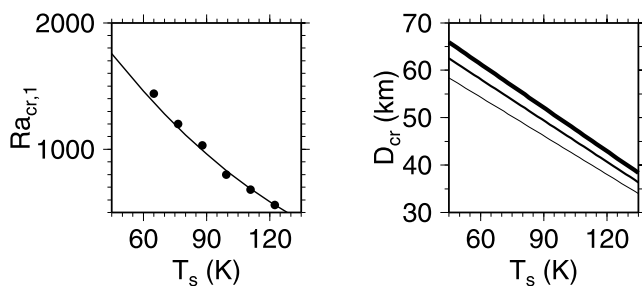


**Figure 4.** (left) Critical Rayleigh number for convection in ice with  $n' = 3.55$  and  $Q^* = 49$  kJ/mol (GSS + dynamic recrystallization) as a function of surface temperature and  $\theta$  for a range of temperatures appropriate for the surfaces of icy satellites. Points indicate values of  $Ra_{cr,1}$  calculated numerically. The line indicates the theoretical values predicted by *Solomatonov* [1995], which can be used to extrapolate our results to higher or lower values of  $T_s$ . (right) Critical ice shell thickness for convection in an ice I shell ( $g = 1.3$  m s $^{-2}$ ) with the GSS rheology and grain sizes given by dynamic recrystallization for  $K = 13$  (thin line) to  $K = 21$  (thickest line).

The equilibration times range from 1 to 10 Myr for values of  $K$  between 13 to 21, and are relatively insensitive to the ice shell thickness because  $D/u_i$  does not depend on ice shell thickness. Therefore it may be impossible to have efficient convective heat transport and well-developed convection in relatively thin ( $D < 40$ – $60$  km) ice shells. In this case, convection could start if the ice grain size were initially small, but convection would be sluggish and limited to a single overturn or small number of overturns occurring before the grain size reaches its equilibrium recrystallized value, at which point the ice would become too stiff to convect. Unimpeded grain growth in a conducting shell [e.g., *Schmidt and Dahl-Jensen*, 2003] could prevent convection from even starting.

### 3. Effect of Impurities

[38] The calculations of ice grain size due to dynamic recrystallization in the ice shells of the satellites we have presented so far suggest that grains in a deforming ice shell will grow to equilibrium sizes of tens of millimeters on timescales of a few million years. Therefore, for convection to occur in ice shells thinner than  $\sim 50$  km [e.g., *McKinnon*, 2006], some process must keep ice grains smaller than a few tens of mm.

[39] Our knowledge of how impurities affect ice grain size comes from examining ice formed during the present interglacial time (the Holocene) and the last glaciation (the Wisconsin). Observations of grain size from many ice cores indicate that grain size decreases across the Holocene-Wisconsin boundary, because of increased levels of non-water ice materials deposited with the ice during the last glacial maximum [e.g., *Gabrielli et al.*, 2004; *Durand et al.*, 2006]. Table 2 summarizes observations of ice grain size in Holocene and Wisconsin ice in the GRIP core, in addition to several other cores in the Arctic and Antarctic. Although the

detailed estimates of ice grain size in clean and dirty ice vary from core to core (clean, interglacial ice has  $d \sim 0.8$  to 4 mm, whereas dusty, cloudy, glacial ice has  $d \sim 0.6$  to 3.5 mm); within each core, grains in impurity-laden ice are invariably smaller than those in clean ice. These values lend support to the “rule of thumb” within the glacial community that ice that looks dirty, cloudy, or bubbly has smaller grains than ice that looks clear and clean [*Alley et al.*, 1986a, 1986b].

[40] Even though general rules about grain size and its variation across pronounced glacial-interglacial boundaries are agreed upon in the literature, the cause of the decrease in grain size and local variations in grain size within interglacial and glacial periods are not completely understood [*Weiss et al.*, 2002]. Similar to dynamic recrystallization, much work exists regarding the effects of second phases on grain growth in metals and rock forming minerals [see *Alley et al.*, 1986a; *Weiss et al.*, 2002, and references therein]. In the absence of impurities, grains grow by grain boundary migration driven by the free energy decrease associated with reduction of grain boundary curvature. Non-water ice materials concentrate on grain boundaries, and exert a drag force on the grain boundary that can slow or even halt grain boundary migration [*Alley et al.*, 1986a, 1986b]. Here we focus on the role played by soluble ions and silicate microparticles, which we consider to be important factors for grain size control in icy satellites.

[41] The role that any type of impurity plays in inhibiting or preventing grain boundary migration in ice depends on where the impurity resides within the microphysical structure of the ice polycrystal. If, for example, micron-sized silicate particles are concentrated along grain boundaries and grain junctions, they can be much more effective at inhibiting grain growth than particles randomly dispersed in the ice [*Durand et al.*, 2006]. We also have the benefit of recent advances in laboratory techniques, chiefly scanning electron microscopy (SEM) [e.g., *Barnes et al.*, 2002; *Ohno et al.*, 2005].

[42] The presence of a non-water cation or anion within an ice crystal generates local strain energy, so it is energetically favorable to push such atomic or molecular impurities

**Table 2.** Observations of Ice Grain Size

Site	Era	Grain Size, mm
GRIP	Wisconsin (Glacial) <sup>a</sup>	2–4
GRIP	Holocene (Interglacial) <sup>a</sup>	4
GRIP	Wisconsin (1980 m) <sup>b</sup>	0.8
GRIP	Holocene (1312 m) <sup>b</sup>	1.2
GRIP	Holocene (cloudy bands) <sup>b</sup>	0.6
GRIP	Holocene (clear sections) <sup>b</sup>	0.9
GRIP	bottom 5 m <sup>c</sup>	3.5
Dome C	Wisconsin <sup>d</sup>	0.9
Dome C	Holocene <sup>d</sup>	2.5
Dome C	Wisconsin (500 m) <sup>b</sup>	1.0
Dome C	Holocene (270 m) <sup>b</sup>	1.4
Devon Island	Wisconsin <sup>d</sup>	0.8
Devon Island	Holocene <sup>d</sup>	1.1
Byrd Station	dusty layer <sup>d</sup>	1.0

<sup>a</sup>*De La Chapelle et al.* [1998].

<sup>b</sup>*Barnes et al.* [2002].

<sup>c</sup>*Tison et al.* [1994].

<sup>d</sup>*Alley et al.* [1986b].

to grain boundaries during recrystallization or grain growth. Concentrations of soluble impurities (such as  $\text{Na}^+$ ,  $\text{Cl}^-$ ,  $\text{Mg}^{2+}$ , and  $\text{SO}_4^{2-}$ ) at the part per million level can, in theory, decrease grain growth rates by an order of magnitude [Alley *et al.*, 1986a]. Before SEM imaging of ice samples, it was generally thought that grain size in Wisconsin ice obtained from Dome C in Antarctica and GRIP was controlled by grain boundary drag caused by soluble ions [Alley *et al.*, 1986b; De La Chapelle *et al.*, 1998]. Recent SEM images, however, show that some ions form salts that sit within ice crystals as coherent inclusions, thus reducing the importance of ion-driven drag forces on grain boundaries [Ohno *et al.*, 2005; Durand *et al.*, 2006].

[43] Micron-sized (and larger) silicate particles also exert a drag force on grain boundaries and may cause grain boundary pinning, where grain growth is slowed or halted altogether because grain boundaries cannot move past the silicate particles. SEM images of ice taken from GRIP and other cores reveal that soluble ions can be more uniformly concentrated in the ice matrix than previously thought, as noted above, which suggests that silicate microparticles may actually control ice grain sizes in the GRIP and other cores [Barnes *et al.*, 2002; Durand *et al.*, 2006]. Detailed microphysical modeling of the drag force of silicate particles on grain boundaries has in fact been able to reproduce ice grain sizes observed in the Wisconsin portion of the Dome C core [Weiss *et al.*, 2002; Durand *et al.*, 2006].

[44] In icy satellites, significant amounts meteoritic and/or primordial dust, dirt, and other particles may be incorporated in their ice I shells, especially in Callisto, whose surface is relatively “dirty” [Moore *et al.*, 2004]. Additionally, the mechanism and timescale of formation of the oceans in icy satellites is not yet clear. Ice forming at the bottom of the ice sheet atop subglacial Lake Vostok, in a relatively quiescent low-stress environment, has grain sizes of order tens of centimeters occurring with large millimeter-sized inclusions [Jouzel *et al.*, 1999]. The contents of the inclusions, mineral deposits and dirt, suggest that pockets of lake water were included in the ice as it froze [Jouzel *et al.*, 1999]. Such an environment may be analogous to the bottom few hundred meters of the ice shell of an icy satellite where melt may intrude into the shell. Because grain growth can be inhibited by particles as small as a few microns, however, we consider it quite plausible that silicate impurities are present in the icy satellites at concentrations at the ppm level (similar to concentrations in the Antarctic Dome Concordia core [Durand *et al.*, 2006]), or even a few tenths of a weight percent (similar to concentrations at GRIP [Tison *et al.*, 1994; De La Chapelle *et al.*, 1998]); Kirk and Stevenson [1987] made such an argument on theoretical grounds (see their Appendix). In addition, clathrates can also pin ice I grain sizes [Durand *et al.*, 2006] because they behave as effectively hard second phases [Durham *et al.*, 2003].

[45] If the volume fraction of dust in the shell is similar to dusty glaciers, of order  $10^{-7}$  to  $10^{-4}$  or so [Alley *et al.*, 1986b; Tison *et al.*, 1994], dust may retard grain growth and keep grain sizes of order 1 mm in the convecting portion of the ice shell. Grain size measurements and concurrent measurements of impurity content in the bottom 5 m of the GRIP ice core show that ice grain size is inversely correlated with the weight percent of impurities and varies

between 2.5 and 4.5 mm [Tison *et al.*, 1994]. Temperatures in the bottom 5 m of the GRIP ice core are greater than 260 K [Thorsteinsson *et al.*, 1997], so grain growth should be fast, and the ice there has experienced significant near-bed shear [Thorsteinsson *et al.*, 1997; De La Chapelle *et al.*, 1998], so dynamic recrystallization may have occurred. This suggests that impurities can retard grain growth and pin grain sizes at values between 2 to 4 mm even in highly deformed ice that is warmed close to its melting point, such as would be found in the interior of a convecting ice I layer. (Thermally activated unpinning of microparticles may also be important on convective timescales [Durand *et al.*, 2006; Gore *et al.*, 1989].)

[46] We have no terrestrial observations or measurements of ice grain size or impurity distribution and migration at the very low temperatures appropriate to icy satellite surfaces. However, determining whether convection is possible, or estimating of the efficiency of convective heat transport, requires knowledge of ice grain size at the base of the ice shell ( $251 \text{ K} < T < 273 \text{ K}$ ), and in the rheological boundary layer between the stagnant lid and the convecting interior (which has a temperature between  $\sim T_i$  and  $T_i - 1.2(n+1)\Delta T/\theta$  [Solomatov and Moresi, 2000], or  $\sim 200\text{--}215 \text{ K}$ ). Given that grain sizes have been measured for dust-bearing polar glacial ice down to  $T \sim 235\text{--}240 \text{ K}$  [De La Chapelle *et al.*, 1998], it is not unreasonable to assume that ice grain size in the convecting interiors of icy satellites may be uniform and close to 1–5 mm.

### 3.1. Can Convection Occur?

[47] If ice grain sizes in the satellites are kept close to 1–5 mm, we expect deformation to occur by a combination of GSS and diffusion creep [Barr *et al.*, 2004; Barr and Pappalardo, 2005; McKinnon, 2006]. For the purposes of this paper we focus on the role of GSS creep. We estimate the conditions under which convection can occur using the relationship between critical ice shell thickness and ice grain size developed for the GSS rheology by Barr *et al.* [2004]. If the strain in ice is accommodated by grain boundary sliding alone, the strain rate is given by equation (5), and the effective viscosity,

$$\eta = \frac{1}{3} \left( \frac{d^p}{A} \right)^{1/n} \dot{\epsilon}_I^{(1-n)/n} \exp\left(\frac{Q^*}{nRT}\right), \quad (20)$$

where  $A$ ,  $n$ , and  $Q^*$  are the laboratory-measured flow constants for ice I, summarized in Table 1. The Rayleigh number at the base of the ice shell is

$$Ra_1 = \frac{3A^{1/n} \rho g \alpha \Delta T D^{(n+2)/n}}{(\kappa d^p)^{1/n} \exp\left(\frac{Q^*}{nRT_m}\right)}. \quad (21)$$

Notice that here the Rayleigh number has an explicit dependence on grain size ( $d$ ) in the denominator because the viscosity due to GSS creep is grain size dependent. For a grain size of 1 mm, the viscosity at the base of the ice shell is  $3 \times 10^{15} \text{ Pa s}$  if the melting temperature of ice is  $T_m = 260 \text{ K}$  and the strain rate is  $1 \times 10^{-13} \text{ s}^{-1}$ . For a grain size

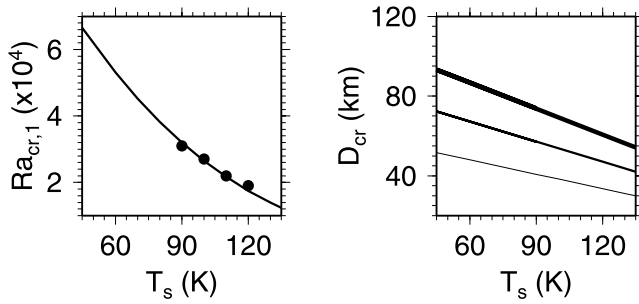


**Figure 5.** (left) Critical Rayleigh number for convection with a GSS rheology, applicable if ice grain size is controlled by the presence of impurities. Circles indicate numerical data from *Barr et al.* [2004], and the line indicates the critical Rayleigh number for convection predicted by *Solomatov* [1995] with a correction factor of 1.5 suggested by the comparison between numerical and theoretical values by *Solomatov and Barr* [2006]. The critical Rayleigh number ranges from  $1.1 \times 10^4$  for  $T_s = 140$  K to  $6.7 \times 10^4$  for  $T_s = 45$  K. (right) Variation in the minimum ice shell thickness where convection is allowed in an ice shell with uniform grain size of 1 mm (thin line), 2.5 mm, and 5 mm (thickest line). Deformation in the ice shell is accommodated by grain-size-sensitive creep [*Goldsby and Kohlstedt*, 2001, 2002], assumed to be due to grain boundary sliding. Values of gravity ( $g = 1.3 \text{ m s}^{-2}$ ) and melting temperature of ice ( $T_m = 260$  K) are chosen to represent average values for a large to midsized pure water ice satellite.

of 5 mm, the viscosity under similar temperature and strain rate conditions is  $10^{16}$  Pa s.

### 3.1.1. Critical Rayleigh Number

[48] The work of *Barr et al.* [2004] characterized the critical Rayleigh number for convection using a grain boundary sliding rheology for ice I for surface temperatures between 90 K and 130 K, generally appropriate for the Galilean satellites, though not in their cold polar regions. To extend the range of surface temperatures to cover these polar regions and surfaces of icy satellites elsewhere in the solar system, we compare the results of the theoretical relationship between  $Ra_{cr}$ ,  $n$ , and  $Q^*$  developed by *Solomatov* [1995] to the numerical results of *Barr et al.* [2004].

[49] Characterization of  $Ra_{cr,1}$  for non-Newtonian fluids by *Solomatov and Barr* [2006] suggests that the theoretical relationship from *Solomatov* [1995] underestimates the minimum value of  $Ra_{cr,1}$  by a factor of  $\sim 1.2$  for  $n = 2$  and effective viscosity contrast across the convecting layer of  $10^{10}$ . Because both *Solomatov* [1995] and *Solomatov and Barr* [2006] use a temperature-linearized flow law, so the mismatch between theory and data is not due to differences in the form of the viscosity function. The differences are likely due to second-order effects not included in the analysis of *Solomatov* [1995]. The adjustment between the theoretical scaling of *Solomatov* [1995] and the numerically derived values is inversely proportional to the viscosity contrast, which controls the extent to which convection is confined to a thin sublayer beneath the stagnant lid: a key

assumption of the analysis of *Solomatov* [1995]. At lower viscosity contrasts, the adjustment between the theoretical and numerically derived values is greater, closer to a factor of  $\sim 1.5$ . The equivalent viscosity contrast across the ice shell in our studies is approximately  $10^5$  to  $10^{10}$ .

[50] Applying a correction factor of  $\sim 1.5$ , and using the definition of  $\theta$  in equation (14), the numerical results of *Barr et al.* [2004] match the theoretical scaling relationship from *Solomatov* [1995], allowing us to extrapolate the results of *Barr et al.* [2004] to lower surface temperatures. Figure 5 (left) shows the critical Rayleigh number as a function of surface temperature for  $T_s = 45$  through  $T_s = 130$  K. The critical Rayleigh number for convection with the GSS rheology varies from  $1.4 \times 10^4$  at  $T_s = 130$  K to  $6.7 \times 10^4$  at  $T_s = 45$  K.

### 3.1.2. Minimum Ice Shell Thickness for Convection

[51] The minimum ice shell thickness where convection can occur can be obtained from the definition of the Rayleigh number as

$$D_{cr} = \left( \frac{Ra_{1,cr} (\kappa d^p)^{1/n} \exp\left(\frac{Q^*}{nRT_m}\right)}{3A^{1/n} \rho g \alpha \Delta T} \right)^{n/(n+2)} \quad (22)$$

Figure 5 (right) shows the variation in minimum ice shell thickness as a function of surface temperature using values of melting temperature and gravity appropriate for a large icy satellite,  $T_m = 260$  K, and  $g = 1.3 \text{ m s}^{-2}$ . The minimum shell thickness where convection occurs varies by a factor of  $\sim 2$  as surface temperature is varied from 45 to 140 K, and varies by a factor of 1.5 as ice grain size increases from 1 to 5 mm. For a grain size of 5 mm, close to values observed in impurity-laden glacial ice, the critical shell thickness for convection ranges from 93 km for  $T_s = 45$  K to 56 km for  $T_s = 130$  K. Comparison of Figures 4 and 5 indicates that convection more or less proceeds in the presence of dynamic recrystallization, despite the much larger average ice grain sizes when recrystallized. The effective grain size in the rheological sublayer (under the stagnant lid), which controls the convective flow [*Solomatov and Moresi*, 2000], is not so large, however (e.g., Figure 3). Moreover, the effective activation energy for flow is  $Q^*/n'$  (equation (11)), much lower than  $Q^*/n$ , markedly reducing the viscosity contrast across the layer.

### 3.2. Convective Heat Flux

[52] The convective heat flux across an ice shell where convective strain is accommodated by GSS creep can be determined from the scaling relationships between  $Nu$  and rheological parameters discussed in section 2.2. Here, we evaluate the scaling relationship for  $Nu$  using  $n = 1.8$ ,

$$Nu = 0.706\theta^{-1.473} Ra_1^{0.474}. \quad (23)$$

Figure 6 shows the variation in  $Nu$  as a function of surface temperature and ice shell thickness for ice grain sizes of 1 mm, 2.5 mm, and 5 mm. With a uniform grain size of 1 mm, the ice shell can convect quite vigorously with  $Nu \sim 7$  for an ice shell thickness of 180 km and a nominal surface temperature of 110 K. If the ice grain size is 5 mm, convection in an ice shell 180 km thick with  $T_s = 110$  K is



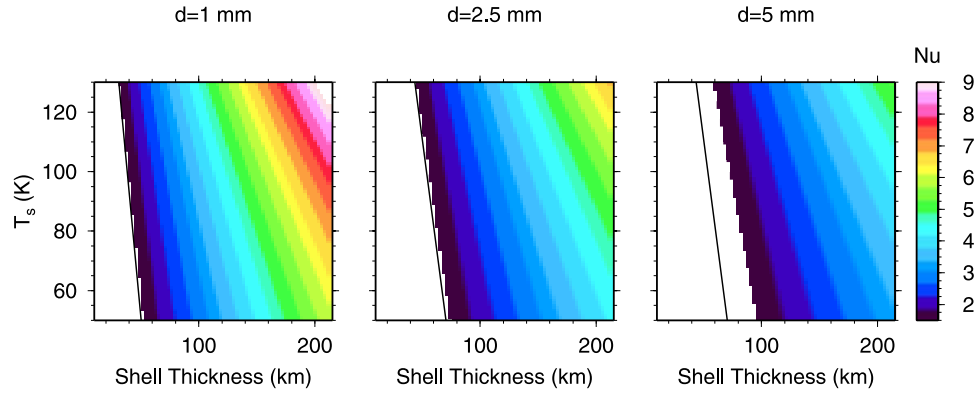


**Figure 6.** Convective heat flux  $Nu$  for convection in an impurity-laden ice shell with uniform grain size of (left) 1 mm, (middle) 2.5 mm, and (right) 5 mm. When the ice grain size is constant at 1 mm, convection is vigorous ( $Nu$  can be as large as  $\sim 7.5$  for  $D = 180$  km, the maximum permitted ice shell thickness in a Ganymede- or Callisto-like satellite), but convective vigor and efficiency of convective heat flux decrease as the ice grain size increases. Lines show the locations of the critical ice shell thickness for convection as a function of surface temperature (see Figure 5).

less efficient, with  $Nu \sim 4$ . We emphasize again that these values are based on the time-dependent scaling given by *Solomatov and Moresi* [2000], and with respect to real icy satellites, do not account for shell curvature or temperature-dependent thermal conductivity (see section 2.2). In addition, as in all non-Newtonian convection, a thermal perturbation of finite amplitude must exist for convection to begin [*Solomatov*, 1995; *Barr et al.*, 2004; *Barr and Pappalardo*, 2005].

#### 4. Summary

[53] The mean grain size in icy satellite mantles and shells is not well constrained. Existing estimates have been developed specifically for Europa’s ice shell and give poor constraints on ice grain size (estimates range from microns to hundreds of meters), because they do not consider physical processes that might control grain size in a realistic ice shell. Terrestrial ice sheets experience strain rate, stress, and temperature conditions similar to the interiors of ice I shells on large to mid-sized icy satellites. Therefore characterization of grain size and models of the microphysical processes that control it can provide constraints on grain size expected in icy satellite interiors. Here we have used information about grain size, ice rheology, dynamic recrystallization, and the role of non-water ice impurities to

generate two end-member models of grain size for the satellites.

[54] In one end-member case, we consider that ice grain size in the satellites is controlled by dynamic recrystallization, where grain size changes as the ice accumulates strain. Using a relationship between recrystallized grain size and stress that reproduces grain sizes in recrystallized metals and rock-forming materials, we are able to construct a microphysically self-consistent relationship between grain size, strain rate, and temperature in the Greenland GRIP ice core. In order to achieve the equilibrium recrystallized grain size predicted by dynamic recrystallization, the ice in the GRIP core and in the satellites’ ice shells and mantles has to have experienced a strain of about 25%. This limits the applicability of the GSS + dynamic recrystallization model to the convecting interior of a satellite’s ice shell and mantle, and also means that our grain size estimates can help determine when convection may be sustained or may turn off in an icy layer, but not whether it can turn on.

[55] Table 3 summarizes the results of the application of our dynamic recrystallization model to a Ganymede- and Callisto-like satellite. When we apply the grain size model

**Table 3.** Summary of Results for a Ganymede- or Callisto-like Satellite

Property	Dynamic Recrystallization	Impurities
Gravity	$1.3 \text{ m s}^{-2}$	$1.3 \text{ m s}^{-2}$
Surface temperature range	45–130 K	45–130 K
Rheology	GSS + dynamic recrystallization	GSS creep
Critical Rayleigh number <sup>a</sup>	$4.8 \times 10^2$ to $1.8 \times 10^3$	$1.4\text{--}6.7 \times 10^4$
Critical shell thickness $D_{cr}$	35–66 km <sup>b</sup>	31–93 km <sup>c</sup>
Equilibrium mean grain size	30–80 mm	1–5 mm
Timescale for convective turnoff	1–10 Myr	–

<sup>a</sup>Values reported for minimum and maximum surface temperature.

<sup>b</sup>Minimum value is for  $K = 13$  and  $T_s = 130$  K, and maximum is for  $K = 21$  and  $T_s = 45$  K.

<sup>c</sup>Minimum value is for  $d = 1$  mm and  $T_s = 130$  K, and maximum is for  $d = 5$  mm and  $T_s = 45$  K.



to outer ice I shells of large icy satellites, we determine that grain sizes within such convecting ice shells should evolve to be relatively large, from 30 to 80 mm. The grain size within a convecting ice shell is heterogeneous and reflects variations in the strain rate and temperature field within the shell. The equilibrium recrystallized grain size in a convecting shell is so large that the ice may become too viscous to convect. In a Ganymede- and Callisto-like satellite, if convection begins in an ice shell with small grain size, ice shells thinner than  $\sim 35$  km will stop convecting in 1–10 Myr, if grain sizes evolve as predicted by dynamic recrystallization in the absence of impurities. Convection in thin shells may be sluggish and possibly limited to one or two convective overturns before stopping altogether, if it starts at all.

[56] Our second end-member model, which yields a lower limit on ice grain size, is based on grain size observed in ice that has modest amounts ( $\sim 10^{-4}$  or less by volume) of non-water ice impurities: silicate microparticles, soluble ions, and clathrates. In dusty, cloudy layers of terrestrial ice sheets, grain size is kept essentially constant by non-water ice impurities that concentrate on grain boundaries and slow or halt grain growth. If grain sizes in the satellites is kept constant at between 1 to 5 mm by non-water ice impurities, convection can be more vigorous than predicted by the dynamic recrystallization model, and can occur in much thinner ice shells. Additionally, provided the soluble ions, and/or silicate particles are incorporated in the ice shells, the timescale over which convection can occur is not limited by grain size evolution; rather, it should be controlled by the heat flux from the interior of the satellite. In tidally flexed ice shells such as on Europa, tidal stress may control grain size, which is a subject of future work.

[57] **Acknowledgments.** This work is supported by a NASA Outer Planets Research Program grant to W. B. McKinnon and has benefitted from discussions with S. Kirby, C. C. Reese, and V. S. Solomatov and reviews by L. Han, F. Nimmo, and G. Tobie.

## References

- Alley, R. B., J. H. Porepezko, and C. R. Bentley (1986a), Grain growth in polar ice: I. Theory, *J. Glaciol.*, **32**, 415–424.
- Alley, R. B., J. H. Porepezko, and C. R. Bentley (1986b), Grain growth in polar ice: II. Application, *J. Glaciol.*, **32**, 425–433.
- Barnes, P. R. F., R. Mulvaney, K. Robinson, and E. W. Wolff (2002), Observations of polar ice from the Holocene and the glacial period using the scanning electron microscope, *Ann. Glaciol.*, **35**, 559–566.
- Barr, A. C., and R. T. Pappalardo (2005), Onset of convection in the icy Galilean satellites: Influence of rheology, *J. Geophys. Res.*, **110**, E12005, doi:10.1029/2004JE002371.
- Barr, A. C., R. T. Pappalardo, and S. Zhong (2004), Convective instability in ice I with non-Newtonian rheology: Application to the icy Galilean satellites, *J. Geophys. Res.*, **109**, E12008, doi:10.1029/2004JE002296.
- De La Chapelle, S., O. Castelnau, V. Lipenkov, and P. Duval (1998), Dynamic recrystallization and texture development in ice as revealed by the study of deep ice cores in Antarctica and Greenland, *J. Geophys. Res.*, **103**, 5091–5106.
- Derby, B. (1991), The dependence of grain size on stress during dynamic recrystallization, *Acta Metall. Mater.*, **39**, 955–962.
- Deschamps, F., and C. Sotin (2001), Thermal convection in the outer ice shell of large icy satellites, *J. Geophys. Res.*, **106**, 5107–5121.
- Dumoulin, C., M.-P. Doin, and L. Fleitout (1999), Heat transport in stagnant lid convection with temperature- and pressure-dependent Newtonian or non-Newtonian rheology, *J. Geophys. Res.*, **104**, 12,759–12,777.
- Durand, G., et al. (2006), Effect of impurities on grain growth in cold ice sheets, *J. Geophys. Res.*, **111**, F01015, doi:10.1029/2005JF000320.
- Durham, W. B., and L. A. Stern (2001), Rheological properties of water ice: Applications to satellites of the outer planets, *Annu. Rev. Earth Planet Sci.*, **29**, 295–330.
- Durham, W. B., S. H. Kirby, and L. A. Stern (2003), The strength and rheology of methane clathrate hydrate, *J. Geophys. Res.*, **108**(B4), 2182, doi:10.1029/2002JB001872.
- Frost, H. J., and M. F. Ashby (1982), *Deformation Mechanism Maps*, 167 pp., Elsevier, New York.
- Gabrielli, P., et al. (2004), Meteoritic smoke fallout over the Holocene epoch revealed by iridium and platinum in Greenland ice, *Nature*, **432**, 1011–1014.
- Goldsby, D. L., and D. L. Kohlstedt (2001), Superplastic deformation of ice: Experimental observations, *J. Geophys. Res.*, **106**, 11,017–11,030.
- Goldsby, D. L., and D. L. Kohlstedt (2002), Reply to comment by P. Duval and M. Montagnat on “Superplastic deformation of ice: Experimental observations,” *J. Geophys. Res.*, **107**(B11), 2313, doi:10.1029/2002JB001842.
- Gore, M. J., M. Grujicic, G. B. Olson, and M. Cohen (1989), The dependence of grain size on stress during dynamic recrystallization, *Acta Metall.*, **37**, 2849–2854.
- Humphreys, F. J., and M. Hatherly (2004), *Recrystallization and Related Annealing Phenomena*, 2nd ed., Oxford Univ. Press, New York.
- Jouzel, J., et al. (1999), More than 200 meters of lake ice above subglacial Lake Vostok, Antarctica, *Science*, **286**, 2138–2141.
- Kirk, R. L., and D. J. Stevenson (1987), Thermal evolution of a differentiated Ganymede and implications for surface features, *Icarus*, **69**, 91–134.
- McKinnon, W. B. (1999), Convective instability in Europa’s floating ice shell, *Geophys. Res. Lett.*, **26**, 951–954.
- McKinnon, W. B. (2006), On convection in ice I shells of outer solar system bodies, with specific application to Callisto, *Icarus*, **183**, 435–450.
- Mitri, G., and A. P. Showman (2005), Convective-conductive transitions and sensitivity of a convecting ice shell to perturbations in heat flux and tidal-heating rate: Implications for Europa, *Icarus*, **177**, 447–460.
- Moore, J. M., et al. (2004), Callisto, in *Jupiter: The Planet, Satellites & Magnetosphere*, pp. 397–426, Cambridge Univ. Press, New York.
- Moore, W. B. (2006), Thermal equilibrium in Europa’s ice shell, *Icarus*, **180**, 141–146, doi:10.1016/j.icarus.2005.09.005.
- Moresi, L., and M. Gurnis (1996), Constraints on the lateral strength of slabs from three-dimensional dynamic flow models, *Earth Planet. Sci. Lett.*, **138**, 15–28.
- Moresi, L.-N., and V. S. Solomatov (1995), Numerical investigation of 2D convection with extremely large viscosity variations, *Phys. Fluids*, **7**, 2154–2162.
- Nimmo, F., and M. Manga (2002), Causes, characteristics, and consequences of convective diapirism on Europa, *Geophys. Res. Lett.*, **29**(23), 2109, doi:10.1029/2002GL015754.
- Ohno, H., M. Igarashi, and T. Hondoh (2005), Salt inclusions in polar ice core: Location and chemical form of water-soluble impurities, *Earth Planet. Sci. Lett.*, **232**, 171–178.
- Poirier, J.-P. (1985), *Creep of Crystals*, Cambridge Univ. Press, New York.
- Rainey, E. S. G., and D. J. Stevenson (2005), Grain size-dependent viscosity and oceans in icy satellites, *Lunar Planet. Sci.* [CD-ROM], **XXXVI**, abstract 2100.
- Reese, C. C., V. S. Solomatov, and L.-N. Moresi (1999), Non-Newtonian stagnant lid convection and magmatic resurfacing on Venus, *Icarus*, **139**, 67–80.
- Ruiz, J., and R. Tejero (2003), Heat flow, lenticulae spacing, and possibility of convection in the ice shell of Europa, *Icarus*, **162**, 362–373.
- Schmidt, K. G., and D. Dahl-Jensen (2003), An ice crystal model for Jupiter’s moon Europa, *Ann. Glaciol.*, **37**, 129–133.
- Schubert, G., T. Spohn, and R. T. Reynolds (1986), Thermal histories, compositions, and internal structures of the moons of the solar system, in *Satellites*, pp. 224–292, Univ. of Ariz. Press, Tucson.
- Schubert, G., J. D. Anderson, T. Spohn, and W. B. McKinnon (2004), Interior composition, structure and dynamics of the Galilean satellites, in *Jupiter: The Planet, Satellites & Magnetosphere*, pp. 281–306, Cambridge Univ. Press, New York.
- Shimizu, I. (1998), Stress and temperature dependence of recrystallized grain size: A subgrain misorientation model, *Geophys. Res. Lett.*, **25**, 4237–4240.
- Solomatov, V. S. (1995), Scaling of temperature- and stress-dependent viscosity convection, *Phys. Fluids*, **7**, 266–274.
- Solomatov, V. S. (2001), Grain size-dependent viscosity convection and the thermal evolution of the Earth, *Earth Planet. Sci. Lett.*, **191**, 203–212.
- Solomatov, V. S., and A. C. Barr (2006), Onset of convection in fluids with strongly temperature-dependent, power-law viscosity, *Phys. Earth Planet. Inter.*, **155**, 140–145.
- Solomatov, V. S., and L.-N. Moresi (2000), Scaling of time-dependent stagnant lid convection: Application to small-scale convection on Earth and other terrestrial planets, *J. Geophys. Res.*, **105**, 21,795–21,818.

- Spohn, T., and G. Schubert (2003), Oceans in the icy Galilean satellites of Jupiter?, *Icarus*, *161*, 456–467.
- Thorsteinsson, T., J. Kipfstuhl, and H. Miller (1997), Textures and fabrics in the GRIP ice core, *J. Geophys. Res.*, *102*, 26,583–26,600.
- Tison, J. L., T. Thorsteinsson, R. D. Lorrain, and J. Kipfstuhl (1994), Origin and development of textures and fabrics in basal ice at Summit, Central Greenland, *Earth Planet. Sci. Lett.*, *125*, 421–437.
- Tobie, G., G. Choblet, and C. Sotin (2003), Tidally heated convection: Constraints on Europa's ice shell thickness, *J. Geophys. Res.*, *108*(E11), 5124, doi:10.1029/2003JE002099.
- Weiss, J., J. Vidot, M. Gay, L. Arnaud, P. Duval, and J. R. Petit (2002), Dome Concordia ice microstructure: Impurities effect on grain growth, *Ann. Glaciol.*, *35*, 552–558.
- Zhong, S. M., M. Gurnis, and L. Moresi (1998), Role of faults, nonlinear rheology, and viscosity structure in generating plates from instantaneous mantle flow models, *J. Geophys. Res.*, *103*, 15,255–15,268.
- Zhong, S. M., M. T. Zuber, L. Moresi, and M. Gurnis (2000), Role of temperature-dependent viscosity and surface plates in spherical models of mantle convection, *J. Geophys. Res.*, *105*, 11,063–11,082.

---

A. C. Barr, Department of Space Studies, Southwest Research Institute, 1050 Walnut Street, Suite 400, Boulder, CO 80302, USA. (amy@boulder.swri.edu)

W. B. McKinnon, Department of Earth and Planetary Sciences, Washington University in Saint Louis, Campus Box 1169, 1 Brookings Drive, Saint Louis, MO 63130-4862, USA.